Analytical Tunnel-boring Machine Pose Precision and Sensitivity Evaluation for Underground Tunnelling

D. Li[a], S. Mao[a], M. Lu[a] and X. Shen[b]

[a]Department of Civil & Environmental Engineering, University of Alberta, Canada
[b]School of Civil and Environmental Engineering, University of New South Wales, Australia
E-mail: duanshun@ualberta.ca, mao1@ualberta.ca, mlu6@ualberta.ca, x.shen@unsw.edu.au

ABSTRACT

Practical Tunnel-boring Machine (TBM) guidance systems usually use sophisticated instruments to obtain the orientation of the TBM. These systems require frequent calibration and work shutdown, making the procedure complex and time consuming. Besides, the majority of current TBM guidance solutions cannot provide the position of the invisible cutter head analytically including commonly used laser point tracking system. This makes it impossible to check the accuracy of the TBM positioning for ensuring the quality of the tunnel being installed in the ground. To address the problem, this research proposes an analytical approach to quantify the accuracy of the TBM position and orientation estimation based on a previously proposed survey-based TBM guidance system. The coordinates for the cutter head center are derived through error propagation based on defining geometric constraints and applying computing algorithms, such as the layout configuration of the prisms mounted on the TBM and the relative position of the cutter head center. The paper also provides a thorough analysis of the sensitivity of the solution with regards to certain configurations based on underlying formulas. To verify the results, a tunnelling experiment was also conducted based on a 1:20 scaled TBM model with its cutter head visible. The proposed method provides a valuable approach to evaluate the accuracy of the cutter head position estimation and potentially enable the operators to control and guide the tunnelling process in the field.

Keywords -

TBM; Navigation; Analytical; Error Propagation, Accuracy; Sensitivity

1 Introduction

Construction is the implementation process in the field, transforming the engineering design into the final product in the real world. In tunnel construction, the design makes rules about start/end locations, depth, tunnel diameter, liner material, and grades; contractor must devise effective methods for both implementing design and checking design in the field in order to satisfy error tolerances in technical specifications. In tunnel construction, the geospatial-related design factors (start/end locations, depth, diameter, and grades) are represented by an invisible as-designed tunnel alignment, and the TBM position is presented by vertical/horizontal offsets (grade/line deviations) from this alignment. TBM guidance systems are responsible to interpret the invisible alignment into visible indicators, and guide the TBM operator steering on the right track. A widely accepted visible indicator is a visible laser beam, which is parallel to the as-designed alignment. Then laser projects at a receiving target mounted on the TBM, therefore the invisible tunnel alignment is marked as a visible laser dot on the target board [1].

The surveyor team of the tunnel construction has two critical tasks: translating the design specification into as-designed alignment for the guidance systems; and checking conformity between the alignment and the indicator given by the guidance system. Due to the complex on-site environment of a tunnel under construction, the guidance system cannot reliably maintain the conformity with the as-designed alignment for a long time period [1]. Both the guidance instructions and steering operations must be well-managed to enable the tunnel's as-built alignment to be fully functional, for either large-diameter traffic tunnels or small-diameter drainage tunnels. For example, when a seriously misaligned TBM breaks through to the exit shaft of a drainage tunnel, the as-built tunnel may not be able connect to existing drainage pipelines. Or a misaligned railway tunnel may cause steeply curved tracks, and trains need to reduce speed to safely pass by [2]. Moreover, if the guidance instructions or the steering operations are not reliable and consistent, the as-built drainage tunnel can be bumpy, which will cause trouble in channelling storm water flow [3]. Therefore, the error at the breakthrough point should generally be controlled with $10mm$ to $20mm$ per $1km$ length for traffic tunnel, and drainage tunnel should not be misaligned more than 150 mm horizontally nor 89 mm vertically at any section of the tunnel being built [4,5].

Surveyors utilize traverse and levelling methods to fix the current horizontal and vertical position of the TBM [2,5,6]. Due to the geometry of tunnelling, both traverse and levelling deals with open-end loop, which means errors in survey cannot be easily detected and compensated [5]. Chrzanowski and Stiros thoroughly studied the errors in traverse and levelling survey on tunnel breakthrough accuracy [2,5]. As surveyors interpret tunnel alignment for guidance systems using the traverse and levelling results, the errors accumulated in survey procedures will introduce errors between as-designed and as-surveyed alignments.

Modern laser-based TBM guidance systems [7] utilize motorized laser to calibrate the parallelism of the laser beam and computerized the processing of receiving targets for attitudes calculation [8–10]. These methods simplify the calibration of laser beam, however, they rely on parallelism between laser and alignment to guide TBM, and they are all affected by the survey errors in the as-surveyed alignment. An improved method, the Virtual Laser Target Board (VLTB) [7,11], attempts to reduce the complexity in navigating the construction of $2.4\sim3\ m$ diameter drainage tunnels. The VLTB system utilizes three-point positioning algorithms [12] to locate the cutter head from three visible prisms situated within a visible window at the rear end of TBM, instead of parallelism of laser beam. VLTB still cannot dodge the errors from survey data, and this paper studies the error model based on three-point positioning algorithm, and provides a valuable approach to evaluate the accuracy of the cutter head position estimation.

2 Theory of Errors

2.1 True Values, Samples, and Errors

A surveying device is supposed to retrieve true measurement values; however, due to all uncontrollable manufacturing and technological limits, the true value cannot be found. Therefore, to calibrate a surveying device, manufacturers should establish a benchmark, utilizing some finer (more accurate) survey equipment. There are two main indicators of the so-called "accuracy" of survey device: accuracy and precision. As shown in Figure 1:

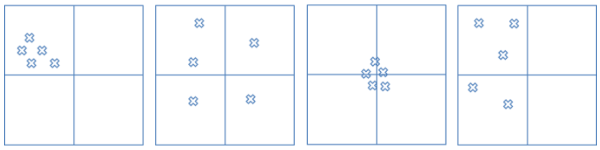

Figure 1 Shooting at the center of the cross: (from left to right) precise not accurate, accurate not precise, accurate and precise, and not accurate not precise

The accuracy suggests the deviation between the average of all measurements and the true value, and precision means the consistency of all measurements. Mathematically, for a set of measurements $X_1 \cdots X_n$ on a true value $\hat{X}$, the accuracy can be quantified by $\left\| \frac{X_1+\cdots+X_n}{n} - \hat{X} \right\|$, and precision can be quantified as standard deviation $\sqrt{\frac{\left(X_1 - \frac{X_1+\cdots+X_n}{n}\right)^2 + \cdots + \left(X_n - \frac{X_1+\cdots+X_n}{n}\right)^2}{n-1}}$ [13].

A well-calibrated survey device should produce unbiased measurements ($\lim_{n\to\infty} \left\| \frac{X_1+\cdots+X_n}{n} - \hat{X} \right\| = 0$), and the precision should be quantified, for instance expressed as standard deviation σ. Later in usage, the device should be able to measure any target with an error, which can be expressed as a normal distributed variable with 0 as mean and σ as standard deviation.

In the following sections, all true values of the targets are not known and errors, either from measurement or error propagation calculation, are expressed as normal distributed variables with 0 as mean and a given standard deviation.

2.2 Error Propagation

In real world survey or other experiments, it is not always practical to directly observe or measure the target, and the unobservable point will be deduced from a set of observable indicators with function models and constraints. For example, the bucket of the excavator is not always observable during construction, and by using kinematics, the bucket position can be deduced from the kinematic chain model plus certain length measurements of hydraulic rods. However, length measurements contain random errors, which in turn will propagate the errors to the kinematic result, through a chain of linear and non-linear computations.

Suppose a set of observations $X = [x_1 \quad \dots \quad x_n]^T$ with a counterpart set of true values as $X^{true} = \left[x_1^{true} \quad \dots \quad x_n^{true}\right]^T$. The true values cannot be directly measured due to random noise, and the random noise fits to a normal distribution(μ,σ), with μ as mean and σ as standard deviation. In order to eliminate random noise, repeat measurements on n variables for m times, and the results are marked as $X^1 \quad ... \quad X^m$. The expectation of these n variables are $E(X)$ and if $m \to \infty$, then $\mu_X = E(X) \to X\hat{}true$. In addition, the covariance of all variables is: $\sigma_{XX} = C_{XX} = \begin{bmatrix} \sigma_{x_1x_1} & \cdots & \sigma_{x_1x_n} \\ \vdots & \ddots & \vdots \\ \sigma_{x_nx_1} & \cdots & \sigma_{x_nx_n} \end{bmatrix}$.

For a set of deduced variables $Z = [z_1 \quad ... \quad z_m]^T$, and $Z = KX + K^0$ with $K = \begin{bmatrix} K_{11} & \cdots & K_{1n} \\ \vdots & \ddots & \vdots \\ K_{m1} & \cdots & K_{mn} \end{bmatrix}$ and $K^0 = [k_1^0 \quad ... \quad k_n^0]^T$ being a linear expression of coefficient K and observable variables X, and K^0 are constants. The expectation, variance-covariance matrix of Z after propagation can be expressed as [13]:

$$E(Z) = E(KX + K^0) = KE(X) + K^0 = K\mu_X + K^0$$

$$C_{ZZ} = KC_{XX}K^T = K\sigma_{XX}K^T$$

As for nonlinear expressions, $Z = \begin{bmatrix} f_1(X_1, \dots, X_n) \\ \vdots \\ f_m(X_1, \dots, X_n) \end{bmatrix}$, with each $f_i(X_1, \dots, X_n)$ as a non-linear function. In this case, the error analysis is performed on local derivable segments, and all functions $f_i(X_1, \dots, X_n)$ need to be linearized at some given point $[x_1^0 \quad ... \quad x_n^0]^T$. Apply total derivative on each function $f_i(X_1, \dots, X_n)$, then $dz_i = \left(\frac{df_i}{dx_1}\right)_0 dx_1 + \cdots + \left(\frac{df_i}{dx_n}\right)_0 dx_n$, therefore the mean and covariance of nonlinear functions at point $[x_1^0 \quad ... \quad x_n^0]^T$ can be expressed as [13]:

$$dZ = K \cdot dX$$

$$dZ = \begin{bmatrix} dz_1 \\ \vdots \\ dz_m \end{bmatrix}, dX = \begin{bmatrix} dx_1 \\ \vdots \\ dx_m \end{bmatrix} \text{ and } K = \begin{bmatrix} \left(\frac{df_1}{dx_1}\right)_0 & \cdots & \left(\frac{df_1}{dx_n}\right)_0 \\ \vdots & \ddots & \vdots \\ \left(\frac{df_m}{dx_1}\right)_0 & \cdots & \left(\frac{df_m}{dx_n}\right)_0 \end{bmatrix}$$

$$\mu_Z = E(Z) = \begin{bmatrix} f_1(E(X_1), \dots, E(X_n)) \\ \vdots \\ f_m(E(X_1), \dots, E(X_n)) \end{bmatrix} \text{ and } \sigma_{ZZ} = KC_{XX}K^T = K\sigma_{XX}K^T$$

3 Analytical Accuracy of TBM Navigation

3.1 Tunnel-boring Machine Three-point Positioning Accuracy

The three-point positioning algorithm for TBM [12] is based on the similar idea as kinematics models, which calculate the coordinates of the target (e.g. the cutter head center) through limited measurable parameters. In a typical three-point positioning problem, the affecting factors include:

- Prior covariance of reference points (installed on the completed tunnel as tunnel survey control points)
- Total station
  - Standard deviation of angle measurement error
  - Standard deviation of distance measurement error
  - Standard deviation of prism-center locating error
  - Parts per million error in distance measurement
- Three-point rotation and transformation
  - Error due to rotation/transformation strategy

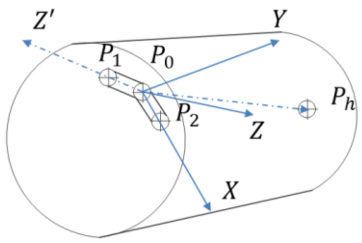

Figure 2 Three measurable points and cutter head

Despite the multiple factors in the above list, the error analysis can be modelled through two steps: 1) determine the covariance matrix for point survey; 2) determine the rotation error due to point survey error.

The total station surveys a target by electronic distance measurement and horizontal/vertical angle measurement. As shown in Figure 3, the slope distance between total station and target is d, and vertical/horizontal angles are θ and α separately. The coordinate of the total station is $Q = \begin{bmatrix} X_Q \\ Y_Q \\ Z_Q \end{bmatrix}$, then the coordinate of the target is $P =$

$\begin{bmatrix} X_Q + \cos(\theta) \cdot d \cdot \cos(\alpha) \\ Y_Q + \cos(\theta) \cdot d \cdot \sin(\alpha) \\ Z_Q + \sin(\theta) \cdot d \end{bmatrix}$. All six parameters $X_Q, Y_Q, Z_Q, d, \theta, \alpha$ contain errors, then applying total derivative to $\begin{bmatrix} dX \\ dY \\ dZ \end{bmatrix} = \begin{bmatrix} \frac{dP_X}{dX_Q} & \cdots & \frac{dP_X}{d\alpha} \\ \vdots & \ddots & \vdots \\ \frac{dP_Z}{dX_Q} & \cdots & \frac{dP_Z}{d\alpha} \end{bmatrix} \begin{bmatrix} X_Q \\ Y_Q \\ Z_Q \\ d \\ \theta \\ \alpha \end{bmatrix} \triangleq D \cdot \begin{bmatrix} X_Q \\ Y_Q \\ Z_Q \\ d \\ \theta \\ \alpha \end{bmatrix}$. Assume the covariance of all six parameters $X_Q, Y_Q, Z_Q, d, \theta, \alpha$ is $C_{X_Q, Y_Q, Z_Q, d, \theta, \alpha}$, then the $C_{XYZ} = D \cdot C_{X_Q, Y_Q, Z_Q, d, \theta, \alpha} \cdot D^T$.

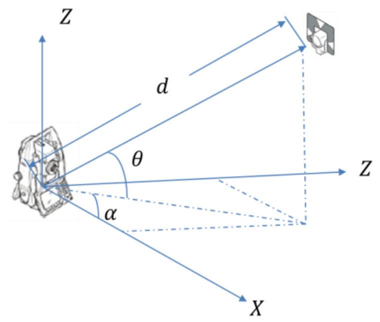

Figure 3 Survey model of total station

In the second step, the total station measures the three visible points P_0, P_1, P_2 with the covariance given above. Before the TBM is taken underground, the relative position between the cutter head and the three visible points is registered in a local coordinate system $P_0 - XYZ$. The coordinate system is established by the following steps (as shown in Figure 2):

- Temporary axis: $Z' \triangleq norm(P_1 - P_0)$
- Axis: $X \triangleq norm(P_2 - P_0)$
- Axis: $Y \triangleq Z' \times X$
- Axis: $Z =\triangleq X \times Y$
- Translation: $T = P_0$
- Rotation matrix: $R = \begin{bmatrix} X^T \\ Y^T \\ Z^T \end{bmatrix}$
- Then there should be $P_h = R(P_h - P_0) + T$

When TBM is taken underground, the robotic total station keeps tracking the three points, and surveys their current coordinates $P_0{}', P_1{}', P_2{}'$. By applying the same coordinate-fixing strategy, the new translation T' and rotation R' can be calculated, and also the current invisible cutter head coordinate is $P_h' = R'(P_h - P_0) + T'$. The coordinate of the cutter head is affected by nine parameters $X_{P_0}, Y_{P_0}, Z_{P_0}, X_{P_1}, Y_{P_1}, Z_{P_1}, X_{P_2}, Y_2, Z_{P_2}$, then the total derivative is $D = \begin{bmatrix} \frac{dX_{P_h'}}{dX_{P_0}} & \cdots & \frac{dX_{P_h'}}{dZ_{P_2}} \\ \vdots & \ddots & \vdots \\ \frac{dZ_{P_h'}}{dX_{P_0}} & \cdots & \frac{dZ_{P_h'}}{dZ_{P_2}} \end{bmatrix}$. The covariance of coordinate of the cutter head can be presented as $C = \begin{bmatrix} \frac{dX_{P_h'}}{dX_{P_0}} & \cdots & \frac{dX_{P_h'}}{dZ_{P_2}} \\ \vdots & \ddots & \vdots \\ \frac{dZ_{P_h'}}{dX_{P_0}} & \cdots & \frac{dZ_{P_h'}}{dZ_{P_2}} \end{bmatrix} \begin{bmatrix} C_{XYZ} & & \\ & C_{XYZ} & \\ & & C_{XYZ} \end{bmatrix} \begin{bmatrix} \frac{dX_{P_h'}}{dX_{P_0}} & \cdots & \frac{dX_{P_h'}}{dZ_{P_2}} \\ \vdots & \ddots & \vdots \\ \frac{dZ_{P_h'}}{dX_{P_0}} & \cdots & \frac{dZ_{P_h'}}{dZ_{P_2}} \end{bmatrix}^T$

4 Sensitivity Analysis

In the real VLTB navigation practice for tunnel construction, two kinds of survey should be done to make it complete. The shop survey aims to find the layout of the three prisms fixed at the end of the TBM and the cutter head. Thus another prism is mounted at the cutter head of the TBM. As the cutter head will not be visible in the tunnel during tunnel construction, the shop survey has to be done before the installation of the TBM. All of the positions of four prisms have to be measured by the total station in this stage. The field survey is used to find the direction of the TBM, or the position of the cutter head in the field coordinate system. Different from shop survey, in the field survey, the cutter head is not measured directly by the total station but through the transformation estimated from the three points at the end of the TBM.

In real tunnel applications, it is not possible to measure the cutter head of the TBM, thus the validation is done in lab with the scaled TBM model with its cutter head center point being visible. The procedure used to evaluate the accuracy is made up of two stages in order to imitate the shop survey and the field survey. In practice, compared to the shop survey, the environment of field survey and the position of the total station in relation to the TBM in the tunnel changes significantly. To make the imitation much more realistic, the position of the total station is moved to another place after the first stage shop survey in lab. After the total station is changed to another location, the total station has to do the resection to set up its own location, just like the case of field survey. The change of location of the total station makes the validation much more realistic, while also introducing additional error caused by the change of environment and the change of the relative position configuration of the total station and the prisms. These changes will affect the accuracy of prism detection and targeting and the accuracy of the total station itself and the measurements. The validation procedure is much different from the case when the same coordinate system is used without moving the total station.

Therefore the system is expected to result in lower accuracy. However the validation is much more reliable and realistic.

In the experiment, two cycles are conducted in each stage and all of the 4 prisms are measured in each cycle; the coordinates of the three prisms at the back end are used for computing the cutter head center while the surveyed coordinate of the cutter head center is used for cross-checking purpose. First, a survey similar to the shop survey for registration of critical points on TBM is done to determine the layout of the prisms. For convenience, it will be referred as shop survey. In the lab setup, the local field coordinate system is defined with a single large prism. The approach is different from the practical case where resection with two known control points is required to determine the location and orientation of the total station in the local field coordinate system, however the difference will be only reflected as a minor translation which does not affect the application.

The geometry layout of the prisms is given in Figure 4. The large prism is used to set the orientation (Northing or Y in the local coordinate system) which can be replaced with any other target. P1, P2, and P3 are three prisms at the end of the TBM (model) and P4 is the prism at the cutter head of the TBM model which is only visible at the mechanical shop for a real TBM. The station point is fixed at coordinates (0.0456, -0.0144, 0.0285) in (East, Northing, Elevation) system for all of the cycles of survey.

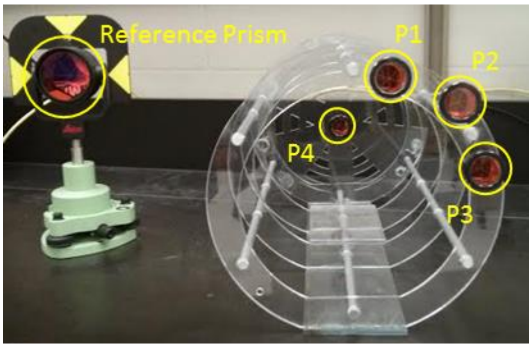

Figure 4 Geometry layout of the prisms

To evaluate the accuracy of the algorithm, measurements of the 4 prisms at 5 different stations are used to simulate the shop survey and field survey alternatively. The data is presented in Table 1. The data collected from different stations were used as shop survey and field survey alternatively to mimic the real application. After the transformation is determined, the coordinates of P4 at the shop survey station is transformed to the field coordinate system. The deviation of the coordinates between the transformed P4 from the shop survey station and the measured P4 at the field survey station were used to evaluate the accuracy of the transform algorithm.

The experiment can be divided into two categories. One category uses single station data to simulate the process, i.e. the data from one station but different cycles will be used to simulate the shop survey and the field survey. In this case, cycle 1 of each station was used as shop survey and cycle 2 was treated as field survey. The other category which is the focus of this study follows the procedure stated in previous sections. This category uses data in different stations to simulate the shop survey and the field survey and thus is much more realistic. In our experiment, the cycle 1 of each station was used as shop survey and field survey alternatively to generate multiple cases. Considering the procedure of calculation has been given in previous

Table 1 Coordinates of $P1 \sim P4$ in Five Different Total Station Setup

Unit (meter)		Station 1			Station 2			Station 3			Station 4			Station 5		
		X	Y	Z	X	Y	Z	X	Y	Z	X	Y	Z	X	Y	Z
Cycle 1	P1	0.408	4.175	-0.204	0.440	4.029	-0.206	0.374	3.787	-0.202	0.406	3.448	-0.205	0.402	3.650	-0.206
	P2	0.468	4.172	-0.227	0.500	4.031	-0.229	0.433	3.777	-0.225	0.467	3.444	-0.228	0.462	3.645	-0.230
	P3	0.491	4.171	-0.288	0.523	4.033	-0.291	0.456	3.774	-0.287	0.490	3.444	-0.289	0.485	3.644	-0.291
	P4	0.425	4.629	-0.318	0.413	4.482	-0.321	0.434	4.236	-0.317	0.426	3.902	-0.319	0.427	4.103	-0.321
Cycle 2	P1	0.408	4.175	-0.204	0.440	4.029	-0.206	0.374	3.787	-0.202	0.406	3.448	-0.205	0.402	3.650	-0.206
	P2	0.468	4.171	-0.227	0.500	4.031	-0.229	0.433	3.777	-0.225	0.467	3.444	-0.228	0.462	3.645	-0.230
	P3	0.491	4.171	-0.288	0.523	4.033	-0.291	0.456	3.774	-0.287	0.490	3.444	-0.289	0.485	3.644	-0.291
	P4	0.425	4.629	-0.318	0.413	4.482	-0.321	0.434	4.236	-0.317	0.426	3.902	-0.319	0.427	4.103	-0.321

sections, only the result will be shown in this section.

Table 2 Error Evaluation

	Station Type		Triad Error (mm)			Quaternion Error (mm)		
	Shop	Field	X	Y	Z	X	Y	Z
Single Station	1	1	12.2	2.2	12.0	12.3	2.2	12.1
	2	2	0.0	0.0	0.0	0.0	0.0	0.0
	3	3	0.0	0.0	0.0	0.0	0.0	0.0
	4	4	0.0	0.0	0.0	0.0	0.0	0.0
	5	5	0.0	0.0	0.0	0.0	0.0	0.0
Vary Stations	1	2	9.1	3.2	10.3	9.2	3.2	10.2
	1	3	12.6	1.0	7.3	12.5	1.1	7.2
	1	4	8.5	2.2	11.8	9.7	2.1	11.5
	1	5	9.8	1.6	7.7	9.5	1.7	7.4
	2	1	-9.2	-2.7	-10.3	-9.4	-2.7	-10.2
	2	3	3.1	-0.4	-3.0	2.8	-0.3	-2.9
	2	4	-0.8	0.0	1.5	0.3	-0.1	1.3
	2	5	0.5	-0.6	-2.6	-0.1	-0.5	-2.8
	3	1	-12.3	-2.7	-7.3	-12.2	-2.7	-7.2
	3	2	-3.1	-0.3	3.0	-2.8	-0.3	2.9
	3	4	-3.9	0.0	4.4	-2.6	0.0	4.2
	3	5	-2.6	-0.5	0.4	-2.8	-0.4	0.2
	4	1	-8.4	-2.7	-11.7	-9.7	-2.7	-11.4
	4	2	0.8	0.1	-1.5	-0.3	0.0	-1.3
	4	3	3.9	-0.5	-4.4	2.5	-0.2	-4.2
	4	5	1.3	-0.6	-4.1	-0.3	-0.5	-4.0

The result shows that the quaternion method does not improve the result very much because no constraints are available to restrict the solution to the real solution if only three prism are used to estimate the transformation. Another finding is that the error can be significant even the total station is not moved according to the result when cycle 1 of station 1 was taken as shop survey and cycle 2 of station 1 as field survey. In this case, the mere difference is the minor difference ($1\,mm$) of P2, however, the result produces quite a large error. To verify this problem, the sensitivity of the algorithm due to the measurement error of each coordinate of the points is evaluated through an analytical approach which calculates the distance between the estimated cutter head and the measured one with varying error on one coordinate of P2. In the experiment, the data collected in cycle 1 at station 1 is used as the shop survey. The field survey data is the cycle 1 data collected at station 1 as well but with a varying minor error added on to the X, Y and Z coordinates separately.

The deviation of the cutter head vs the error in the coordinates of the surveyed points is given in Figure 5 to Figure 13. The gradient of the curve at 0 will be the partial derivative of the Y value corresponding to the X value which can be found in the Jacobian matrix derived in previous sections.

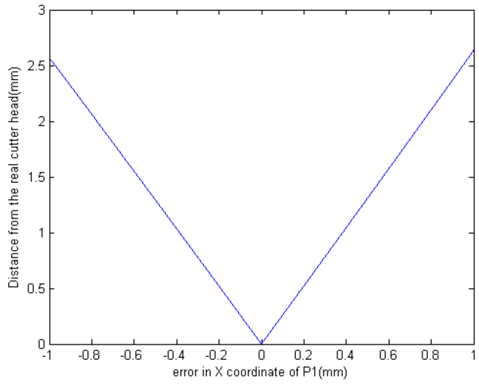

Figure 5 Deviation vs error of X coordinate of P1

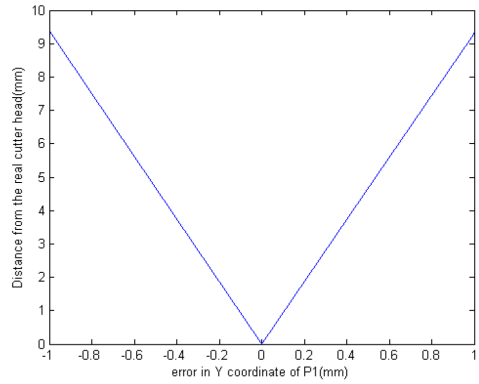

Figure 6 Deviation vs error of Y coordinate of P1

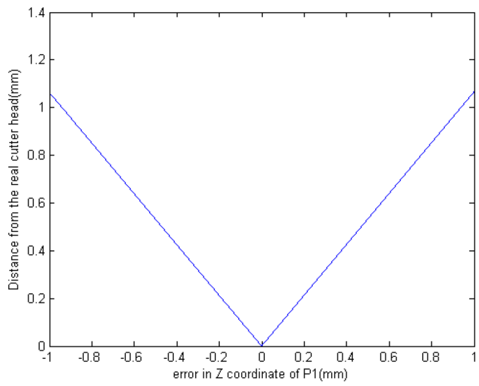

Figure 7 Deviation vs error of Z coordinate of P1

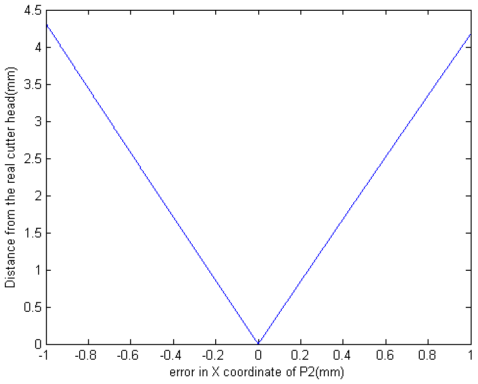

Figure 8 Deviation vs error of X coordinate of P2

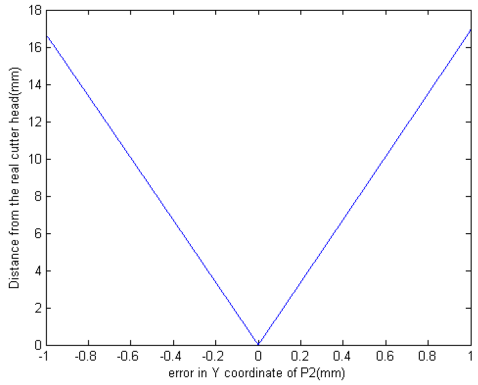

Figure 9 Deviation vs error of Y coordinate of P2

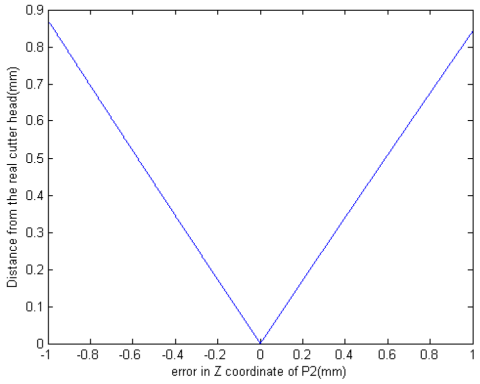

Figure 10 Deviation vs error of Z coordinate of P2

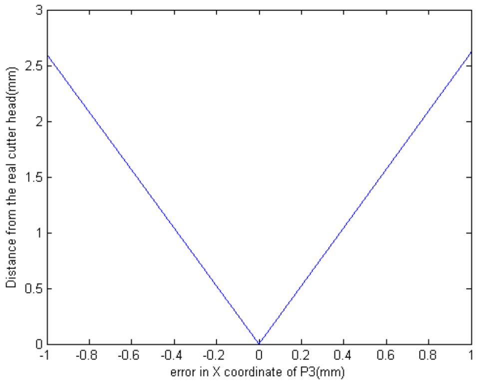

Figure 11 Deviation vs error of X coordinate of P3

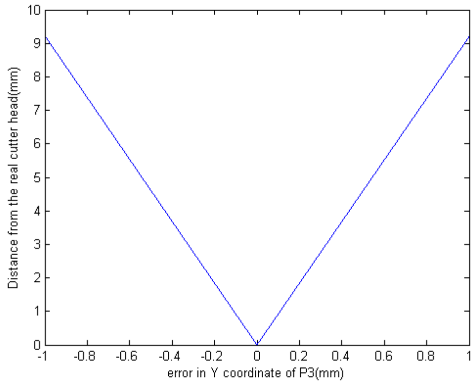

Figure 12 Deviation vs error of Y coordinate of P3

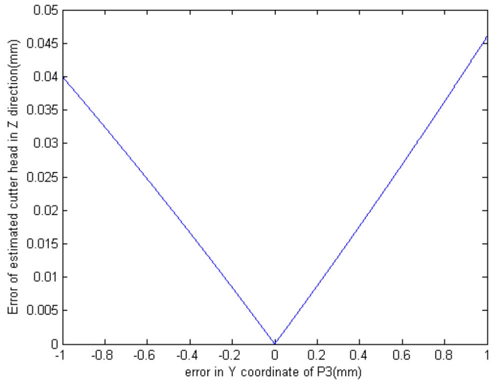

Figure 13 Deviation vs error of Z coordinate of P3

Based on results, it is observed that the measurement error of the Y coordinate of P2 has the largest influence on the result under the geometry layout of the TBM model. A 1 mm error on the Y coordinate of P2 can result in as large as 18 mm error in the position error of the estimated cutter head. The error in Y direction of P1 and P3 can reach as high as 10 mm error as well. To further analyse the error, it is split in X, Y and Z directions separately, the result with measurement error in Y coordinate of P2 is given in the following figures.

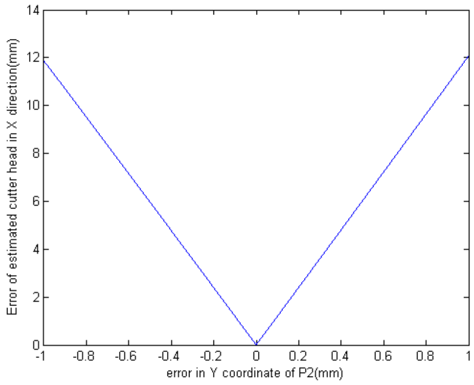

Figure 14 Deviation of cutter head on X direction vs error of Z coordinate of P3

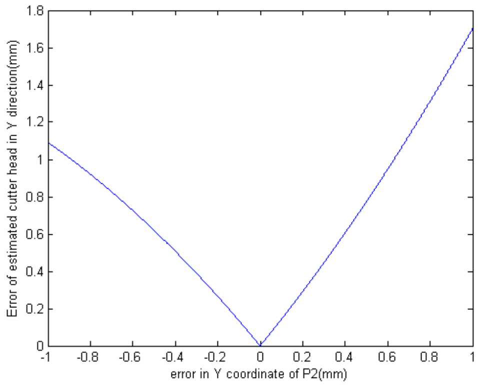

Figure 15 Deviation of cutter head on Y direction vs error of Z coordinate of P3

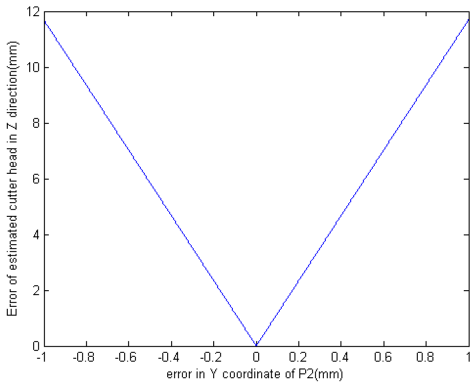

Figure 16 Deviation of cutter head on Z direction vs error of Z coordinate of P3

However, the error along the direction of the as-design tunnel should be ignored because what is critical is the alignment error on the plane perpendicular to the direction of the as-design tunnel alignment. Usually an alignment tolerance will be set for the tunnel depending on the application. To ensure the quality of the tunnel construction and analyse the sensitivity of the algorithm in term of alignment error, the positioning error is projected on to the plan by assuming that the current direction where the TBM is heading to is exactly the direction of the as-built design.

Based on the assumption, the alignment error will be:

$$\boldsymbol{e} \times (\boldsymbol{P_4} - \boldsymbol{C})$$

Where $\boldsymbol{C}$ is the rear center of the TBM which can be derived from P1, P2, and P3; $\boldsymbol{e}$ is the deviation of the estimated cutter head compared to the measured cutter head. The alignment error corresponding to errors on Y direction of P2 is given in Figure 17. From the figure it can be concluded that the error in Y coordinates of P2 would result in a large error of the cutter head and most of the error will contribute to the alignment error which is critical to tunnel construction.

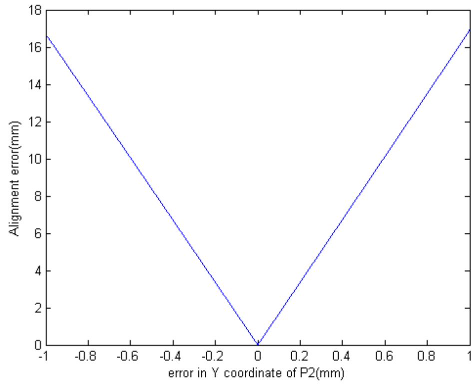

Figure 17 Alignment error vs error of Y coordinate of P2

5 Conclusions

The paper discusses the system-wide error sources and propagation model of three-point positioning algorithm for TBM guidance. To better simulate the different environments of shop registration and site survey in real world case, the validation test relocates the total station after initial coordinate registration, and calculates the error from the new location. The result shows that, given three known prisms, the quaternion method will not have better result than the triad method, as there is no redundant survey to adjust errors.

In the sensitivity analysis, due to the short distances between prisms, even $1\,mm$ error on $Y - axis$ would result in $18\,mm$ error in cutter-head position calculation. Although this error is large and reflects the difficulty to estimate the cutter-head from a small survey window, the error along the direction of the as design tunnel should be ignored because what really matters is the alignment error on the plane perpendicular to the direction of the as design tunnel alignment. Moreover, the error is independent between every two surveys, and the error will not accumulate. This means the error in deviation measurement is well controlled and the deviation measurement is reliable.

In the future, the authors will optimize the geometry of the setup of the prisms, and introduce a fourth prism as a survey redundant to further improve the accuracy for cutter head estimation.

References

[1] Mao S and Shen X and Lu M and Wu X. Real-time Tablet-based Virtual Reality Implementation to Facilitate Tunnel Boring Machine Steering Control in Tunnel Construction. Proceedings of 13th International Conference On Construction Applications of Virtual Reality, London, United Kingdom, 2013.

[2] Stiros SC. Alignment and Breakthrough Errors in Tunneling. Tunnelling and Underground Space Technology. (24). 236–44, 2009.

[3] Wu X and Lu M and Mao S and Shen X. Real-time As-built Tunnel Product Modeling and Visualization by Tracking Tunnel Boring Machines. The Proceedings of 30th International Symposium of Automation and Robotics in Construction and Mining (ISARC 2013) Proceedings, Montreal, Canada, 2013.

[4] The City of Edmonton. The City of Edmonton - Design & Construction Standards - Volume 3: Drainage 2012.

[5] Chrzanowski A. Optimization of The Breakthrough Accuracy in Tunneling Surveys. The Canadian Surveyor. (35). 5–16, 1981.

[6] Kavanagh BF. Surveying with Construction Applications. Upper Saddle River, N.J., Prentice Hall, 2010.

[7] Shen X and Lu M. Development of Virtual Laser Target Board for Tunnel Boring Machine Guidance Control. Computing in Civil Engineering (2012), American Society of Civil Engineers, 2012, pages 413–20.

[8] Jardón A and Victores JG and Martínez S and Balaguer C. Experience Acquisition Simulator for Operating Microtuneling Boring Machines. Automation in Construction. (23). 33–46, 2012.

[9] tacs GmbH. Tacs Acs +++ Summary of The Acs Guidance System 2004. http://www.tacsgmbh.de/en/tacs_prod_acs_overview.htm (accessed May 2, 2013).

[10] VMT GmbH. SLS-T APD Tunnel Guidance System 2003.

[11] Mao S and Shen X and Lu M. Virtual Laser Target Board for Alignment Control and Machine Guidance in Tunnel-Boring Operations. Journal of Intelligent & Robotic Systems. 1–16, 2014.

[12] Shen X and Lu M and Chen W. Computing Three-Axis Orientations of A Tunnel-Boring Machine Through Surveying Observation Points. Journal of Computing in Civil Engineering. (25). 232–41, 2011.

[13] Mikhail EM and Ackermann FE. Observations and Least Squares, with Contributions by F. Ackermann. New York, IEP, 1976.